

ISSN 0011-1643

UDC-541.1

CCA-2070

Original Scientific Paper

Geometrical Restrictions of Incoherent Transport of Water by Diffusion in Protein of Silica Fineparticle Systems and by Flow in a Sponge. A Study of Anomalous Properties Using an NMR Field-Gradient Technique

Franz Klammler and Rainer Kimmich

Universität Ulm, Sektion Kernresonanzspektroskopie, W-7900 Ulm, Germany

Received September 10, 1991

Geometrical restrictions of incoherent water transport in different aggregated particle systems and in a natural sponge were studied using an NMR field gradient technique. Two series of experiments were carried out.

First, the temperature and concentration dependences of the water diffusion coefficient were measured in aqueous systems of bovine serum albumin and gelatin above and below the bulk-water freezing temperature. The concentrations ranged from dilute solutions to almost dry powders being only partly hydrated. The diffusion coefficient within clusters of overlapping hydration shells is reduced by one order of magnitude compared with that of bulk water. Geometrical restrictions manifest themselves (a) by the obstruction effect observed at high water concentrations, (b) by the topologically two-dimensional diffusion in the network of overlapping hydration shells, and (c) by the percolation threshold appearing at about 15 %_{b.w.} water.

The second series of experiments indicated geometrical restrictions in the sense that the transport behaviour in some special systems turned out to be anomalous. Hydrated protein aerogels were produced by means of a lyophilization/rehydration procedure. For comparison, hydrated silica fineparticles having a similar diameter as the proteins were investigated in addition. In both cases, the spin-echo decays by diffusion suggest anomalous behaviour. The same conclusion was drawn for water percolating through the pores of a natural sponge, *i.e.* for an incoherent flow process.

INTRODUCTION

Transport in systems with disordered geometrical restrictions is a field related to biological, aggregated, fractal, or amorphous systems. Theoretical concepts developed in terms of fractal dimensions and percolation clusters are of particular interest in this context.¹ One of the motivations which led to this study was to find experimental in-

dications of disordered restrictions and to learn the appropriate description of such systems by well-defined parameters. Here, the term 'transport' particularly means diffusion and (incoherent) flow of water. The investigated systems were proteins, monodisperse silica fineparticles and a natural sponge.

The translational diffusion characteristics of water molecules in aqueous protein systems are expected to deviate from those of bulk water for two reasons. First, there are at least two physically distinguishable phases, *viz.* free and hydration water. The latter is defined and revealed by a much lower solidification temperature.^{2,3} The high mobility of hydration water, even far below the freezing point of bulk water, was demonstrated by diffusion and NMR relaxation studies.^{4,5} For instance, the water content at which the hydration shells in bovine serum albumin (BSA) solutions are saturated was determined as $c_s \approx 30\%_{\text{b.w.}}$ (by weight).⁴ Generally, one expects the displacement rates in the hydration layers to be different from those in free water. If the exchange between the two phases is fast at the time scale of the experiment, the diffusion coefficients are averaged correspondingly.

The second point refers to the obstruction imposed on the diffusion pathways of water molecules by the presence of macromolecules, which form comparatively immobile obstacles. The obstruction effect in dilute solutions was discussed by Wang⁶ and by Clark *et al.*⁷

In weakly hydrated systems, the restriction of diffusion pathways by macromolecules tends to be more complicated. Aggregation clusters may occur, so that fractal properties might have to be taken into consideration.^{1,8,9} The fraction of time spent in the hydration water phase increases with the protein concentration. Therefore, the surface structure of the macromolecules increasingly influences the diffusion behaviour as the water content decreases (apart from the principal reduction of the dimensionality of the diffusion process.). In the terminology of fineparticle science,¹⁰ it is the influence of the texture rather than of the structure of the agglomerate that becomes dominant.

Further reduction of the water content leads to discontinuities of the hydration layers so that the protein surfaces are no longer covered completely. Finally, a »percolation threshold« of the hydration water is expected, as first discussed by Careri *et al.*¹¹

Hydrated aggregates of monodisperse silica fineparticles and porous media, such as a sponge, are considered to belong to the same class of systems. Molecular dynamics again is expected to be governed by disordered restricted geometries.¹²

Particle diffusion on percolation clusters has been already studied by computer simulations.⁹ However, to our knowledge, direct experimental investigations of this problem have not been attempted so far. Other studies related to this field, but of a quite different background, refer to the interpretation of electron-spin resonance (ESR) relaxation data by fracton properties of the density of states¹³ or to the discussion of surface fractality based on NMR relaxation data.¹⁴

A question of particular interest is under which circumstances diffusion in systems with disordered geometric restrictions satisfies the linear Einstein relationship of the mean square displacement and time

$$\langle r^2 \rangle = 6Dt \quad (1)$$

with a single diffusion coefficient D or a distribution of diffusion coefficients. Anomalous diffusion, on the other hand, obeys⁹

$$\langle r^2 \rangle = \alpha t^\kappa \quad (2)$$

with $\kappa \neq 1$. α is a proportionality constant corresponding to the diffusion coefficient in a normal case. With incoherent flow, equivalent transport coefficients are expected.

METHOD

Field-gradient Technique

Diffusion data were measured by means of the NMR field-gradient technique, employing stimulated echoes.¹⁵ The RF-pulse sequence is

$$90^\circ - \tau_1 - 90^\circ - \tau_2 - 90^\circ - \tau_1 - \text{echo} \quad (3)$$

Field-gradients are effective in the two τ_1 intervals, whereas the τ_2 interval is insensitive to the presence of any gradients. Relaxation losses in the τ_1 and τ_2 intervals refer to the transverse and longitudinal magnetization components, respectively.

Stationary fringe-field gradients of superconducting magnets¹⁶ were used. The width of each of the effective gradient intervals is designated by δ . The diffusion time is essentially given by the time delay from the middle of one to the middle of the next effective gradient interval. It is denoted by Δ . In the case of stationary gradients, the width of a gradient interval is $\delta \equiv \tau_1$ and the diffusion time is $\Delta = \tau_1 + \tau_2$.

The attenuation of the spin-echo amplitude A by translational diffusion characterized by Eq. (2) is generally represented by¹⁷

$$A = A_0 \exp \left\{ - \frac{\gamma^2 g^2 \alpha}{3(\kappa + 1)(\kappa + 2)} \left[\frac{1}{2} (\Delta + \delta)^{\kappa+2} + \frac{1}{2} (\Delta - \delta)^{\kappa+2} - \Delta^{\kappa+2} - \delta^{\kappa+2} \right] \right\} + C \quad (4)$$

A_0 is the echo amplitude in the absence of gradients, *i.e.* without influence of translational diffusion (but attenuated by relaxation, of course). g is the field gradient and γ the gyromagnetic ratio. C is a constant taking into account potential baseline offsets and/or quasi constant signal contributions.

Choosing $\kappa = 1$ and equating $\alpha = 6D$ leads to the standard formula valid for normal diffusion for $\tau_2 \gg \tau_1$ ^{15,18}

$$A = A_0 \exp \{ -\gamma^2 D g^2 \delta^2 \Delta \} + C \quad (5)$$

Aqueous protein systems are heterogeneous, *i.e.* molecules with different diffusion properties contribute to the detected signals. Therefore, diffusion decays tend to be non-exponential. In the simplest case, the decays can be described by linear combinations of the expression in Eq. (5) for different diffusion parameters.

Evaluation of Fringe-field Gradient Experiments

The diffusion (or incoherent flow) parameters D and α , κ were determined by fitting the right-hand expressions of Eq. (5) and (4), respectively, to the experimental decay curves after correction for relaxation. The data could be well represented in this way. The constant parameter particularly took into account the signal contributions of immobile or quasi immobile constituents of the samples. As macromolecules can be

considered as such constituents, the diffusion parameters finally determined are designated as *average water diffusion parameters* (D_w , α_w , κ_w) of the protein solution.

With the fringe-field method, the quantities to be varied are the intervals τ_1 or τ_2 . Therefore, the relaxation decays had to be taken into account, explicitly. This was done by using iteration procedures.

In the standard fringe-field experiment, the average water diffusion coefficient D_w or the average water diffusion parameters α_w and κ_w were evaluated from the τ_1 dependence of the echo-amplitude, keeping the diffusion time Δ constant. Two sets of echo-amplitude decays were measured, one with an almost negligible and one with a long τ_2 interval.

In the first series of experiments, the transverse-relaxation decay during the τ_1 intervals was determined by varying τ_1 and keeping the diffusion time Δ as short as possible, so that the influence of diffusion was weak. Practically, the τ_2 interval was chosen to be 30 μ s only, so that $\Delta = \tau_1 + 30 \mu$ s. (Note that the free-induction signals decayed in less than 30 μ s because of the strong field gradients).

Then, a second series of measurements was performed with a diffusion time in a range $\Delta = 1$ to 50 ms. First-order diffusion parameters were evaluated by correcting the echo-amplitude data by the first-order relaxation decay determined in the first step. (The influence of longitudinal relaxation during τ_2 is minor because of the long T_1 times and was considered to be constant for a given Δ value.

The first-order diffusion parameters determined in this way were then used to evaluate the transverse relaxation decay in the second approximation, referring to the echo amplitude data for the short τ_2 interval again. The result is a second-order transverse-relaxation decay. These data served for correction of the echo-amplitude decays for long τ_2 values, yielding second-order diffusion parameters. The whole procedure was repeated in four iteration steps so that, finally, fourth-order water diffusion parameters were available.

In some of the fringe-field experiments the diffusion decays had to be represented as the echo amplitude versus the diffusion time Δ keeping $\tau_1 \equiv \delta$ constant. Therefore, the decay curves were corrected for the influence of longitudinal relaxation. This was done again by using a second set of experimental data recorded with varying τ_2 intervals, but constant and very short τ_1 intervals in this case. The correction of the diffusion decays was carried out iteratively in analogy to the procedure described above.

INSTRUMENTS AND SAMPLES

The fringe-field measurements were carried out with the magnets of a Bruker BMT 47/40 (4.7 T) tomograph and a Bruker MSL 300 (7 T) spectrometer. The magnetic flux densities and their gradients at the measuring positions in the fringe fields were 2.14 T, 9.04 T/m and 2.89 T, 38.4 T/m, respectively, with a stability better than $5 \cdot 10^{-8} \text{h}^{-1}$. The proton resonance frequencies were 81 MHz and 123 MHz, respectively. The gradients were estimated with a GaAs Hall probe or deduced from the variation of the local field values determined by NMR. The gradients were calibrated with the help of the known diffusion coefficient of bulk water. The 90° RF pulse length was 1 to 2 μ s.

Due to the limited RF bandwidth, slices rather than the whole samples (diameter 10 mm) were excited in the presence of the field gradients. Their widths were in all cases much greater than the maximal root mean square displacement of the molecules. Diffusion into or out of the excited slice was, therefore, negligible during the diffusion time Δ .

Bovine serum albumin (BSA, 100 % electrophoretic purity) was purchased from Behringwerke, Marburg, Germany. Gelatin from bovine skin (≈ 225 Bloom) was provided by Sigma, Deisenhofen, Germany. The protein powders were vacuum dried overnight and rehydrated afterwards. Water contents $c_w < 40\%_{b.w.}$ were reached by spreading the powdery material and exposing it, for a longer or shorter period of time, to an atmosphere saturated with water vapor. Solutions in the range $c_w \geq 50\%_{b.w.}$ were produced by direct mixing with neutral distilled water (without buffer). The intermediate range, $40\%_{b.w.} \leq c_w \leq 50\%_{b.w.}$, was covered by wetting the protein spread on a cold aluminium plate with condensing water vapor. All concentrations were determined by weighing the total water uptake. The residual water¹⁹ in the vacuum dried proteins was neglected. The gelatin samples were annealed at 38 °C for one hour after sealing the sample tubes.

Porous protein samples were produced by quenching liquid solutions as fast as possible to nitrogen temperature, lyophilizing them for two weeks, and rehydrating the extremely porous protein material again in an atmosphere saturated with water vapor. Because of the high porosity of this material, it will be called »protein aerogel«. Three BSA solutions with water contents between 50 and 70%_{b.w.} were treated in this way. The water content after rehydration was 35%_{b.w.}, so that the hydration shells were saturated but the free-water was still negligible.

Monodisperse fine silica particles were purchased as a commercial product ('Alfasil', silicon(IV)oxide, 99.8%, No 89376, Johnson Matthey GmbH, Alfa Products, Karlsruhe, FRG). The specific surface was 400 m²/g. The diameter of the particles was specified as 7 nm. The samples were prepared by exposing the dry powder to a moist atmosphere. Water contents up to 50%_{b.w.} could be thus produced. The moistened powder was slightly compressed in sample tubes.

For the incoherent flow experiments, a natural sponge, order horn sponges, was inserted in a 10 mm glass tube. Compression of the sponge was avoided so that the original extension of the pores was maintained. The flow velocity along the main water flow direction was 5 mm/s. This direction was adjusted perpendicular to the field-gradient direction, so that the measurements refer to displacements by incoherent flow perpendicular to the main (predominantly coherent) flow.

RESULTS WITH PROTEIN SOLUTIONS

Diffusion Decays

In principles, one can distinguish protons in free water, hydration water and in proteins. Diffusions in the free water and hydration water phases are more or less completely averaged by the exchange during diffusion time (compare Ref. 4). Distinguishable components, are, therefore, expected only for water in general (fast decay) and for the macromolecules (slow decay).

At temperatures at which free water is frozen but hydration water is still liquid, diffusion decays turn out to be monoexponential, indicating immobilization of the macromolecules. In this case, the only molecules able to diffuse translationally are located in the »infinite« percolation cluster formed by the hydration water shells. Equivalent observations were made with myoglobin single crystals⁵ and myoglobin solutions.²⁰

The principal question is whether water diffusion in protein solutions has an anomalous nature Eq. (2). The answer was given by experiments with BSA solutions where the τ_1 interval was kept constant and the τ_2 interval was varied. Figure 1 shows exemplary decays of the echo amplitude versus the diffusion time Δ . The data are corrected for spin-lattice relaxation and the signal contribution quasi independent of Δ , *i.e.* the component due to the macromolecules, is already subtracted. The solid lines correspond to fits of Eq. (4). The result is that the κ values are close to 1, *i.e.* diffusion behaves normally above as well as below the freezing temperature of free water. The root mean square displacements were $\langle r^2 \rangle^{1/2} \geq 400\text{nm}$ in this experiment.

Indications of an anomalous diffusion behaviour were, however, found with the protein aerogel structures. Experiments with such systems will be described in the next section.

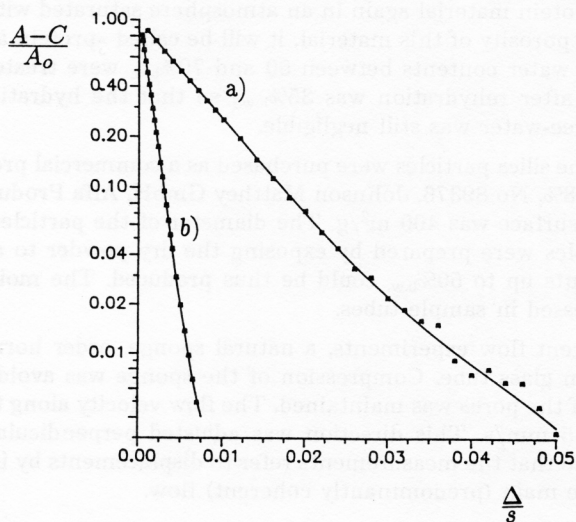


Figure 1. Exemplary spin-echo decays of an aqueous BSA solution ($c_w = 50\%_{b.w.}$) above and below the freezing temperature of free water. The data were measured using the fringe-field method by varying τ_2 . The decay is corrected for the influence of relaxation. Constant or quasi constant signal contributions have been subtracted. The solid lines represent fits of Eq. (4) to the experimental data.

Experimental parameters:

- a) 293 K; $g = 9.04 \text{ T/m}$; $\tau_1 = 160 \mu\text{s}$
 b) 265 K; $g = 38.4 \text{ T/m}$; $\tau_1 = 100 \mu\text{s}$.

Fitted curve parameters:

- a) $\alpha = 3.3 \times 10^{-9} \text{ m}^2/\text{s}^\kappa$; $\kappa = 0.98$.
 b) $\alpha = 1.4 \times 10^{-9} \text{ m}^2/\text{s}^\kappa$; $\kappa = 1.03$.

Temperature Dependence

The temperature dependence of the average diffusion coefficient of aqueous myoglobin solutions with different water contents was already reported in Ref. 20. At high water contents, freezing of free water results in a concentration dependent decay of the diffusion coefficient. No concentration dependence was observed in the frozen

state. This indicates that the hydration water is still liquid at the minus Celsius temperatures investigated and that the hydration shells form »infinite« percolation clusters, permitting displacements from hydration shell to hydration shell.

The data obtained for water concentrations less than saturation concentration⁴ do not indicate any change at the water freezing temperature. They can rather be described by a simple Arrhenius law in the whole temperature range. The conclusion is that the water phase in this case consists solely of hydration water. Therefore, the diffusion coefficients measured at this water content reflect the displacement properties within the hydration shells. The values of the diffusion coefficients are remarkably high and indicate strong translational degrees of freedom of hydration water. This corroborates the equivalent conclusion for water inherently incorporated in sperm whale myoglobin single crystals.⁵

We made several attempts to isolate protein molecules or small protein aggregates in frozen samples by quenching diluted BSA solutions ($c_w > 90\%_{b.w.}$) by means of liquid nitrogen. In all cases, the translational diffusion remained observable at temperatures at which free water was frozen but hydration water was still liquid. The root mean square displacements exceeded the protein diameter by at least one order of magnitude, indicating protein aggregates of corresponding extensions. The explanation is a phase separation process which is still much faster than the freezing rate reached in our experiments. Actually, the diffusion coefficients measured in the frozen solutions were independent of the concentration of the samples and of how fast they were quenched.

Concentration Dependence

Figure 2 shows the dependence of the average water diffusion coefficient on the concentration c_p of BSA or gelatin at room temperature. These data were measured using the fringe-field method. Two breaks are visible at $c_p \approx 50\%_{b.w.}$ and at $c_p \approx 85\%_{b.w.}$, respectively.

The concentration dependence of the water diffusion coefficient is changed by freezing, *i.e.* immobilizing free water while hydration water is still liquid. This is demonstrated in Figure 3. (The water diffusion coefficient D_w refers to the liquid water phases only, of course.)

At 270 K, when free water is already frozen, the concentration dependence vanishes for protein concentrations $c_p < 60\%_{b.w.}$. This indicates that the hydration shell clusters formed in the freezing process are of the same nature, independent of the concentration. Their dimensions also exceed the root mean square displacements during diffusion time. For concentrations $c_p > 60\%_{b.w.}$, a formal decrease is observed, like in the case of temperatures above the freezing point.

Interpretation

Water diffusion in aqueous protein systems is determined by several effects. These become obvious and can be best discussed in terms of concentration dependences (Figure 2).

Range I ($0 \leq c_p < \approx 50\%_{b.w.}$). This case may be characterized as the »free-water limit«. The so-called obstruction effect dominates the concentration dependence. The quasi-static macromolecules form obstacles for the translational diffusion of water molecules, which are mainly in the free-water phase. In the limits of dilute solutions, the expression (compare Refs. 4-7)

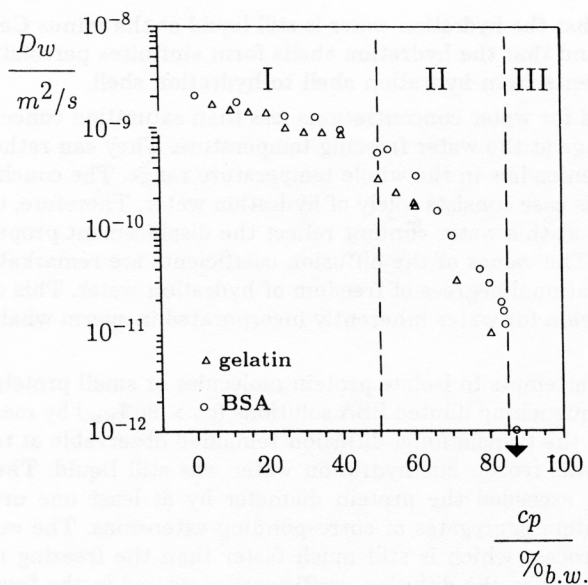


Figure 2. Dependence of the average water diffusion coefficient D_w in aqueous BSA and gelatin solutions on the protein concentration $c_p = 100\% - c_w$: The diffusion decays were measured using the fringe-field method. The τ_1 intervals were varied in the range $25 \mu\text{s}$ to $200 \mu\text{s}$. The diffusion times were $\Delta = 10 \text{ ms}$ and 20 ms with the BSA and the gelatin experiments, respectively. The temperature was 20°C . The data point for $c_p = 87\%_{\text{b.w.}}$ BSA (marked by an arrow) represents the lower limit of the measuring range if the transverse relaxation times $T_2 < 1 \text{ ms}$. No diffusion decay could be measured at this concentration. Therefore, the actual water diffusion coefficient at this concentration must be less than $10^{-12} \text{ m}^2/\text{s}$. Three concentration ranges can be distinguished: $0 \leq c_p < \approx 50\%_{\text{b.w.}}$ (I); $\approx 50\%_{\text{b.w.}} < c_p < \approx 85\%_{\text{b.w.}}$ (II); $\approx 85\%_{\text{b.w.}} < c_p < 100\%_{\text{b.w.}}$ (III).

$$D_w = D_o \frac{1 - \beta\Phi}{1 - \Phi} \quad (6)$$

provides a good description (D_o , diffusion coefficient without obstruction; Φ , volume fraction of the macromolecules; β , shape factor).

Range II ($\approx 50\%_{\text{b.w.}} < c_p < \approx 85\%_{\text{b.w.}}$). With higher protein concentrations, the fraction of hydration water, p_h , increases at the expense of the free water content, $p_f = 1 - p_h$. The exchange between the two water phases takes place at a rate greater than 10^3 s^{-1} and is therefore fast compared with the diffusion time Δ in the experiments.⁴ Hence, the water diffusion coefficient can be written as a weighted average of the diffusion coefficients in free water, D_f , and in the hydration water phase, D_h . (The effective coefficient D_h refers to the three-dimensional Euclidian space while the actual displacements take place in the topologically two-dimensional protein surface layers). Eq. (6) is replaced by

$$D_w = p_h D_h + p_f D_f \quad (7)$$

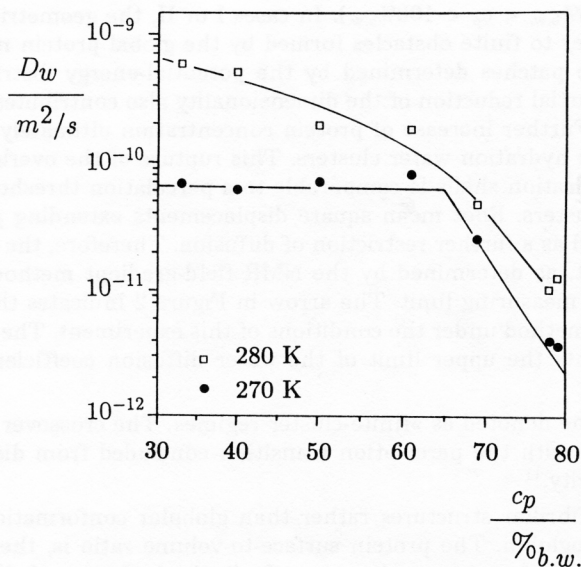


Figure 3. Concentration dependence of the (liquid) water diffusion coefficient D_w of aqueous BSA solutions above and just below the freezing temperature of free water. $\Delta = 20$ ms.

To be detectable, the NMR field-gradient technique requires root mean square displacements much larger than the protein dimension. The fact that measurements of the effective diffusion coefficient are possible, indicates that the hydration water shells are in close contact with one another in this concentration range and overlap at low water contents. Thus, one may speak of the »infinite-cluster regime«.

D_h can be estimated from the plateau value of the 270 K data in Figure 3. Extrapolating to 293 K by means of the water activation energy²¹ of 18 kJ/mol leads to $D_h \approx 1.2 \cdot 10^{-10} \text{ m}^2/\text{s}$. The probability to find a water molecule in the free-water phase is⁴

$$p_f = \frac{c_{ps} - c_p}{(1 - c_p)c_{ps}} + \frac{(1 - c_{ps})c_p}{(1 - c_p)c_{ps}} \cdot \frac{1}{1 + e^{\Delta G/RT}} \quad (c_p \leq c_{ps}) \quad (8)$$

and

$$p_f = \frac{1}{1 + e^{\Delta G/RT}} \quad (c_p \geq c_{ps}) \quad (9)$$

(c_{ps} , protein concentration at which saturation of the hydration shells is reached; ΔG , difference of the molar Gibbs free energy between free and hydration water). Combining Eqs. (6) to (9) and using $\Delta G/RT = 8$ (Ref. 4) and $D_f = 2.2 \cdot 10^{-9} \text{ m}^2/\text{s}$ permits a fit to the experimental data in range II. A saturation concentration $c_{ps} = 0.65$ is in agreement with the value 0.7 derived from NMR relaxation data.⁴ Note, however, that for protein concentrations above this value, D_h cannot be considered constant any more. Consequently, the description of the experimental data in this range by the above formalism is poor.

Range III ($\approx 85\%_{b.w.} < c_p < 100\%_{b.w.}$). In cases I or II, the geometrical restrictions of the diffusion refer to finite obstacles formed by the global protein molecules or by inaccessible surface patches determined by the potential-energy distribution on the protein surfaces. Partial reduction of the dimensionality also contributes to the restrictions of diffusion. Further increase of protein concentration ultimately leads to finite rather than infinite hydration water clusters. This rupture of the overlap of the more or less filled up hydration shells is comparable to a percolation threshold between infinite and finite clusters. Root mean square displacements extending protein dimensions are suppressed as a further restriction of diffusion. Therefore, the effective water diffusion coefficient, as determined by the NMR field-gradient method, tends to become less than the measuring limit. The arrow in Figure 2 indicates the lowest value measurable by our method under the conditions of this experiment. The corresponding data point represents the upper limit of the water diffusion coefficient at this concentration.

This case may be denoted as »finite-cluster regime«. The crossover between cases II and III coincides with the percolation transition concluded from dielectric studies of proton conductivity.¹¹

Gelatin forms fibrillar structures rather than globular conformations like in the case of BSA or myoglobin. The protein surface-to-volume ratio is, therefore, greater and the probability p_h of a water molecules to be in the hydration shells is higher for a given protein concentration. Hence, the reduced values of the water diffusion coefficients in gelatin solutions (Figure 2) and the shifted I \leftrightarrow II crossover, appear to be plausible in the light of the interpretation outlined above.

COMPARATIVE EXPERIMENTS WITH BSA AEROGELS

Water diffusion in aqueous protein systems underlies geometrical restrictions due to the presence of protein molecules and due to the hydration effect. Nevertheless, the diffusion behaviour, is practically normal under the experimental conditions of the field-gradient technique. This is demonstrated by the almost monoexponential decays shown in Figure 1.

The situation is different with the protein aerogels. The lacunary structure of these systems imposes additional restrictions on the water diffusion pathways. In this case, nonexponential water diffusion curves were observed. An example is presented in Figure 4.

The fit of equation (4) to these data leads to an exponent $\kappa = 0.76$ instead of 1. This result was found to be independent of the concentration of the original BSA solution in the investigated range.

The data of Figure 4 were measured with a field gradient of 9.04 T/m. With the higher fringe-gradient of 38.4 T/m, a diffusion time scale of only 0.1 to 10 ms is relevant in the experiments. Therefore, a shorter length scale of the displacements is probed. The result of such experiments was an exponent $\kappa = 0.46$, *i.e.* the anomaly is stronger with lower mean square displacements. This indicates that the origin of the nonexponentiality is not due to ordinary restrictions of diffusion (*e.g.* 22) because then the opposite tendency would be expected.

An explanation based on any heterogeneity of the samples that might lead to a distribution of the water diffusion coefficients would also be problematic. In this case, the dependence of the echo amplitudes on the quantity $g^2\Delta$ should be independent of

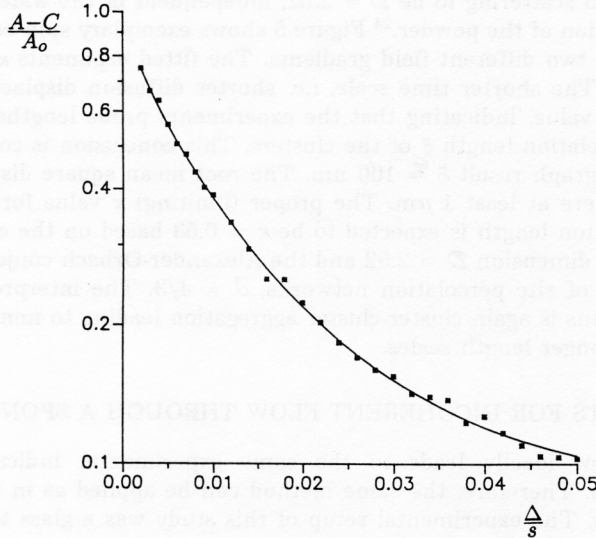


Figure 4. Exemplary spin-echo decay of a hydrated BSA aerogel ($c_w = 35\%_{b.w.}$). The data were measured by varying τ_2 . The decay is corrected for the influence of relaxation. Constant or quasi constant signal contributions have been subtracted. The experimental parameters are: 296 K; $g = 9.04 T/m$; $\tau_1 = 160 \mu s$. The sample was prepared from a BSA solution with an original water concentration $c_w = 60\%_{b.w.}$, as described in the text. The solid line represents a fit of Eq. (4) to the experimental data. The fitted parameters are $\alpha = 9.7 \times 10^{-10} m^2/s^\kappa$; $\kappa = 0.76$.

the actual choice of g . This is not the case: A small g value combined with correspondingly large Δ times produces results different from the opposite choice.

The interpretation of the nonexponential decay curves by anomalous diffusion on self-similar structures, on the other hand, anticipates independence of κ of the diffusion time. This is the essence of the scaling law Eq. (2). However, this equation is valid only for fractal lattices in length scales below the correlation length of the clusters. Thus, a possible conclusion is that the correlation length of the self-similar clusters was already exceeded in the experiments with the lower field gradient, while the result obtained with the high field gradient approaches the prediction for site percolation clusters, namely an exponent $\kappa = 0.57$ (9).

Another rather plausible interpretation is that the structures are not strictly self-similar. The influence of cluster-cluster aggregation effects, for instance, is expected to lead to different behaviour.⁸

RESULTS WITH HYDRATED MONODISPERSE SILICA FINEPARTICLES

Similar results were found with ramified aggregates of colloidal SiO_2 particles commercially known as 'Alfasil'. In their case, principally no signal can arise from the substrate particles bearing the adsorption layers. Therefore, any artifact due to evaluation of the signal contribution of the diffusing molecules is excluded.

The particles form aggregates the fractal dimension of which was determined by small-angle neutron scattering to be $\mathcal{D} = 2.52$, independent of the water content and even after compaction of the powder.²⁴ Figure 5 shows exemplary spin-echo decay curves measured with two different field gradients. The fitted exponents κ are 0.81 and 0.69, respectively. The shorter time scale, *i.e.* shorter diffusion displacements, again leads to a lower κ value, indicating that the experiments probe lengths more or less exceeding the correlation length ξ of the clusters. This conclusion is corroborated by the electron micrograph result $\xi \approx 100$ nm. The root mean square displacements in the experiments were at least $1 \mu\text{m}$. The proper (limiting) κ value for length scales within the correlation length is expected to be $\kappa = 0.53$ based on the experimentally determined fractal dimension $\mathcal{D} = 2.52$ and the Alexander-Orbach conjecture⁹ for the fracton dimension of site percolation networks, $\bar{d} = 4/3$. The interpretation of the depicted observations is again cluster-cluster aggregation leading to non-Euclidian behaviour at much longer length scales.

RESULTS FOR INCOHERENT FLOW THROUGH A SPONGE

Incoherent flow ideally leads to the same experimental indications as the Brownian diffusion. Therefore, the same method can be applied as in the above diffusion experiments. The experimental setup of this study was a glass tube (diameter

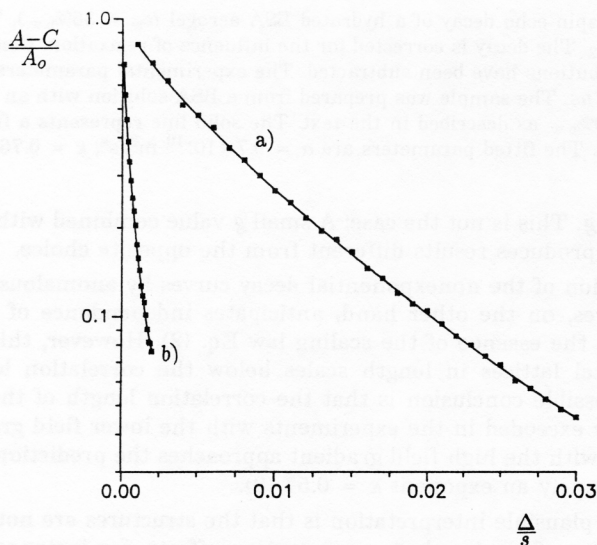


Figure 5. Exemplary spin-echo decays of hydrated silica fineparticle aggregates ('Alfasil', $c_w = 35.8\%_{b.w.}$). The data were measured at 296 K by varying τ_2 while $\tau_1 = 100 \mu\text{s}$ was kept constant. The decays are corrected for the influence of relaxation. Constant or quasi constant signal contributions have been subtracted. The solid line represents a fit of Eq. (4) to the experimental data.

Parameters:

a) $g = 9.04 \text{ T/m}$; $\alpha = 5.7 \times 10^{-9} \text{ m}^2/\text{s}^{\kappa}$; $\kappa = 0.81$; b) $g = 38.4 \text{ T/m}$; $\alpha = 1.4 \times 10^{-9} \text{ m}^2/\text{s}^{\kappa}$; $\kappa = 0.69$.

10 mm) filled with natural sponge, through which water was percolating. The main flow direction was adjusted perpendicular to the direction of the field gradient so that the influence of coherent displacements was considerably suppressed. The irregular displacement components in the field gradient direction through the pores of the sponge can then be considered to be of incoherent nature.

Figure 6 shows the spin-echo decay curve for incoherent flow. The fit of Eq. (4) leads to an exponent $\kappa = 0.24$, *i.e.* an extraordinarily low value. This must be compared with $\kappa = 2$ for ideally coherent flow. If the flow is turned off but the sponge is still filled with water, the transport behaves almost normally. The fitted exponent is then $\kappa = 0.9$.

The nonexponentiality of the decay curve may also be discussed in terms of different water mobilities.²⁵ A fraction of the water might be in more or less isolated pores where the flow is prevented. This non-flowing water is called 'static'. Two coefficients for normal Brownian diffusion, D_{stat} , and for incoherent flow displacement, D_{inc} , must then be considered. The mean square displacement is assumed to be

$$\langle r^2 \rangle = (\alpha_1 D_{\text{inc}} + \alpha_2 D_{\text{stat}}) t \quad (10)$$

where α_1 and α_2 are constants implying the corresponding fractions. The dashed line (b) in Figure 6 is an attempt to describe the spin-echo decay on this basis. The coefficients are $D_{\text{stat}} = 2.1 \cdot 10^{-9} \text{ m}^2/\text{s}$, *i.e.* the mean diffusion coefficient when the flow is turned off, and $D_{\text{inc}} = 3.6 \cdot 10^{-8} \text{ m}^2/\text{s}$.

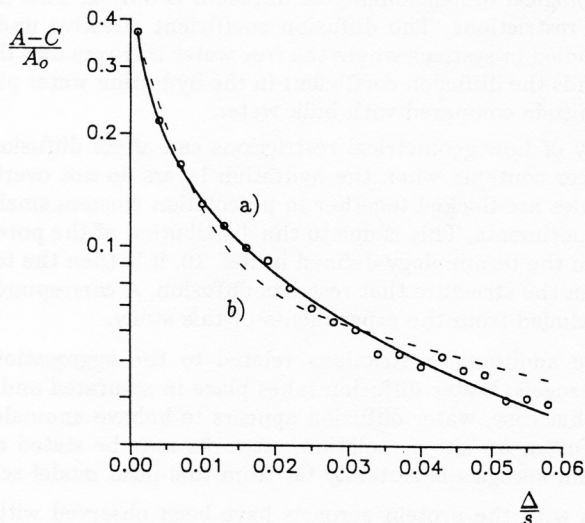


Figure 6. Spin-echo decay for incoherent water flow through the pores of a natural sponge. The main flow velocity was 5 mm/s. The field gradient was perpendicular to the main-flow direction so that only incoherent displacement components along the field gradient influence the decay curve. The data were measured by varying τ_2 , keeping $\tau_1 = 100 \mu\text{s}$ constant. The decays are corrected for the influence of relaxation. Constant or quasi constant signal contributions have been subtracted. The solid line (a) represents a fit of Eq. (4) to the experimental data. The parameters are $g = 9.04 \text{ T/m}$; $\alpha = 8.5 \times 10^{-9} \text{ m}^2/\text{s}^\kappa$; $\kappa = 0.24$. For the meaning of the dashed line (b) see text.

The description of the experimental data by the two-water fraction model is obviously worse than that obtained assuming a single sort of water which underlies anomalous transport: The standard deviation is even 14 times larger.

DISCUSSION

A series of different systems has been studied imposing disordered and ramified geometrical restrictions on displacements of water by diffusion or incoherent flow. A variety of phenomena has been found that reflect these restrictions in a pronounced way.

The results obtained with aqueous protein systems have been interpreted by means of two water phases, namely free and hydration water. The reality of a physically distinguishable hydration water phase is obvious in the light of the different solidification properties. These are revealed, for instance, in the diffusion of water observable under conditions when free water is already frozen. At temperatures above the freezing temperature of free water, diffusion in both phases is effective.

Geometrical restrictions of water diffusion in protein systems are manifested in four different ways. First, there is the obstruction effect which was already observed with dilute solutions in previous studies. Then, there is the diffusion within the hydration water phase taking place with a different diffusion coefficient. With macroscopically liquid samples, the rapid exchange between the two water phases leads to an average diffusion coefficient. There are, however, indications that the microscopic displacement of water molecules within the hydration layers is guided by the protein surfaces so that the topological dimensionality of diffusion is only 2. This is the second effect of geometrical restrictions. The diffusion coefficient effective under such circumstances can be studied in systems where the free water is frozen and the hydration shells overlap. One finds the diffusion coefficient in the hydration water phase reduced by one order of magnitude compared with bulk water.

A third possibility of how geometrical restrictions can affect diffusion properties is relevant at low water contents when the hydration layers do not overlap anymore and the water molecules are flocked together in percolation clusters smaller than the length scale of the experiments. This is due to the distribution of the potential energy on protein surfaces. In the terminology defined in Ref. 10, it is then the texture of the geometries rather than the structure that restricts diffusion. A corresponding percolation threshold is concluded from the experiments of this study.

Finally, there are additional restrictions related to the aggregation properties relevant in protein aerogels. Water diffusion takes place in saturated and overlapping hydration shells. In that case, water diffusion appears to behave anomalously. A certain similarity to diffusion on site-percolation networks may be stated although the structure of the protein aerogels is certainly far from this ideal model scheme.

Similar effects as with the protein aerogels have been observed with aggregated and hydrated monodisperse silica fineparticles and even with incoherent flow through the pores of a natural sponge. In all cases, there are clear indications of anomalous transport behaviour. The conclusions fit the results of nuclear magnetic relaxation studies of porous systems revealing fractal properties.²⁶⁻²⁹

Acknowledgements. – We thank B. Fundel for preparing the samples and the Deutsche Forschungsgemeinschaft for financial support.

REFERENCES

1. J. Feders, *Fractals*, Plenum Press, New York 1988.
2. I. D. Kuntz, *J. Amer. Chem. Soc.* **93** (1971) 514.
3. I. D. Kuntz and W. Kauzmann, *Adv. Protein Chem.* **28** (1974) 239.
4. R. Kimmich, T. Gneiting, K. Kotitschke, and G. Schnur, *Biophys. J.* **58** (1990) 1183.
5. K. Kotitschke, R. Kimmich, E. Rommel, and F. Parak, *Progr. Coll. Polym. Sci.* **83** (1990) 211.
6. J. H. Wang, *J. Amer. Chem. Soc.* **76** (1954) 4755.
7. M. E. Clark, E. E. Burnell, N. R. Chapman, and J. A. M. Hinke, *Biophys. J.* **39** (1982) 289.
8. F. Family and D. P. Landau, (Eds.), *Kinetics of Aggregation and Gelation*, Elsevier, Amsterdam 1984.
9. R. Orbach, *Science* **231** (1986) 814.
10. B. H. Kaye, *A Random Walk Through Fractal Dimensions*, VCH, Weinheim 1989.
11. G. Careri, A. Giansanti, and J. A. Rupley, *Proc. Nat. Acad. Sci.* **83** (1986) 6810.
12. J. Klafter and J. M. Drake, (Eds.), *Molecular Dynamics in Restricted Geometries*, John Wiley, New York 1989.
13. H. J. Stapleton, J. P. Allen, C. P. Flynn, D. G. Stinson, and S. R. Kurtz, *Phys. Rev. Lett* **45** (1980) 1456.
14. D. Fushman, *J. Biomol. Struct. Dyn.* **7** (1990) 1333.
15. J. E. Tanner, *J. Chem. Phys.* **52** (1970) 2523; Erratum: *ibid.* **57** (1972) 3586.
16. R. Kimmich, W. Unrath, G. Schnur, and E. Rommel, *J. Magn. Reson* **12** (1991) 136.
17. J. Kärger, H. Pfeifer, and G. Vojta, *Phys. Rev.* **A37** (1988) 4514.
18. J. Kärger, H. Pfeifer and W. Heink, *Adv. Magn. Reson.* **12** (1988) 1.
19. E. R. Andrew, D. J. Bryant, T. Z. Rizvi, *Chem. Phys. Letters* **95** (1983) 463.
20. R. Kimmich, F. Klammler, V. D. Skirda, I. A. Serebrennikova, A. I. Maklakov, and N. Fatkullin, *Appl. Magn. Reson.*, in press.
21. R. Mills, *J. Phys. Chem.* **77** (1973) 685.
22. P. T. Callaghan, *Aust. J. Phys.* **37** (1984) 359.
23. T. A. Witten and L. M. Sander, *Phys. Rev. Letters* **47** (1981) 1400.
24. S. K. Sinha, T. Fretloft, and J. Kjems, in Ref. 8, page 87.
25. D. Le Bihan, E. Breton, D. Lallemand, P. Grenier, E. Cabanis, and M. Laval-Jeantet, *Radiology* **161** (1986) 401.
26. K. S. Mendelson, *Phys. Rev.* **34** (1986) 6503.
27. F. Devreux, J. P. Boilot, F. Chaput, and B. Sapoval, *Phys. Rev. Lett.* **65** (1990) 614.
28. R. Blinc, G. Lahajnar, S. Žumer, and M. M. Pintar, *Phys. Rev.* **B38** (1988) 2873.
29. R. Blinc, O. Jarh, A. Zidansek, and A. Blinc, *Z. Naturforsch.* **44a** (1989) 163.

SAŽETAK

Geometrijska ograničenja nekoherentnog transporta vode difuzijom proteina ili finih čestica silike te pomoću toka u spužvi

F. Klammler i R. Kimmich

Geometrijska ograničenja nekoherentnog transporta vode u različitim sustavima agregiranih čestica i u prirodnoj spužvi proučavana su tehnikom NMR gradijenta polja. Načinjene su dvije serije eksperimenata. Prvo, temperaturne i koncentracijske ovisnosti difuzijskog koeficijenta vode mjerene su u vodenim sustavima bovin serum albumina i želatine, iznad i ispod temperature smrzavanja glavnine vode (bulk-water). Koncentracije su se kretale od razrijeđenih otopina do gotovo suhih prašaka, samo lagano hidratiziranih. Difuzijski koeficijent unutar nakupina hidratacijskih ljuski, koje se prekrivaju, reduciran je za red veličine u usporedbi s onima za glavninu vode. Geometrijska ograničenja pokazuju se (a) zaprečavajućim (opstrukcijskim) efektom opaženim pri višim koncentracijama, (b) topološkom dvo-dimenzijском difuzijom hidratacijskih ljuski, koje se prekrivaju, i (c) perkolacijskim pragom koji se pojavljuje pri 15% vode.

Druga serija eksperimenata indicirala je geometrijska ograničenja, tako da je transportno ponašanje u nekim specijalnim sustavima postalo anomalno. Hidratizirani proteinski aerogelovi bili su pripremljeni s pomoću liofilizacijsko/rehidracijske procedure. Za usporedbu bile su ispitivane i fine čestice hidratiziranog kvarca, koje imaju sličan promjer kao i proteini. U oba slučaja, gašenje spinske jeke posredstvom difuzije upućuje na anomalno ponašanje. Sam zaključak izveden je za vodu koja perkolira kroz pore prirodne spužve, tj. za nekoherentni proces strujanja.